J|A|C|S
ARTICLES
Published on Web 05/26/2005

# A Study of the Mechanism and Kinetics of Cyclooctene Epoxidation Catalyzed by Iron(III) Tetrakispentafluorophenyl Porphyrin

Ned A. Stephenson and Alexis T. Bell*

*Contribution from the Chemical Sciences Division, Lawrence Berkeley Laboratory and Department of Chemical Engineering, University of California, Berkeley, California 94720-1462*

Received November 2, 2004; E-mail: bell@cchem.berkeley.edu

***Abstract:*** A study has been conducted of the mechanism and kinetics of cyclooctene epoxidation by hydrogen peroxide catalyzed by iron(III) tetrakispentafluorophenyl [$F_{20}$TPPFe(III)] porphyrin. The formation of cyclooctene oxide, the only product, was determined by gas chromatography, and the consumption of hydrogen peroxide was determined by $^1$H NMR. UV−visible spectroscopy was used to identify the state of the porphyrin as a function of solvent composition and reaction conditions and to follow the kinetics of porphyrin degradation. $F_{20}$TPPFe(III) was found to be inactive in the chloride-ligated form, but became active when the chloride ligand was replaced by a methoxide ligand. The methoxide-ligated form of $F_{20}$TPPFe(III) reacts with hydrogen peroxide to form an iron(III) hydroperoxide species, which then undergoes both heterolytic and homolytic cleavage to form iron(IV) $\pi$-radical cations and iron(IV) oxo species, respectively. The iron(IV) $\pi$-radical cations are responsible for the epoxidation of cyclooctene, whereas the iron(IV) oxo species are responsible for hydrogen peroxide decomposition. The kinetics of cyclooctene epoxidation and hydrogen peroxide decomposition developed from the proposed mechanism describe the experimentally observed kinetics accurately. The rate parameters derived from a fit of the model to the experimental data are consistent with previous estimates of the magnitude of these parameters.

## Introduction

Metalloporphyrins are effective catalysts for the selective oxidation of hydrocarbons and other organic compounds under mild conditions.[1−3] As a consequence, considerable effort has been devoted to investigating the effects of variables, such as the composition of the porphyrin, the oxidant, the solvent, and the substrate. The literature pertaining to the use of iron porphyrins in combination with hydrogen peroxide is particularly extensive,[1−24] and a number of studies have been undertaken aimed at identifying the composition of the active species.[1−32] It is suggested that the reaction of hydrogen peroxide with the native iron(III) porphyrin results in the formation of an iron(III) hydroperoxide species,[13] which can then undergo homolytic cleavage to form iron(IV) oxo species or heterolytic cleavage to form iron(IV) $\pi$-radical cations, and all three of these species have been cited as being active for the oxidation of hydrocarbons.[5,6,13,19,21,33,34] However, notwithstanding the many studies

(1) Sheldon, R. A. *Metalloporphyrins in Catalytic Oxidations*; Marcel Dekker: New York, 1994.
(2) Montanari, F.; Casella, L. *Metalloporphyrins Catalyzed Oxidations*; Kluwer Academic Publishers: Boston, MA, 1994.
(3) Meunier, B. *Biomimetic Oxidations Catalyzed by Transition Metal Complexes*; Imperial College Press: London, 1999.
(4) Strukul, G. *Catalytic Oxidations with Hydrogen Peroxide as Oxidant*; Kluwer Academic Publishers: Boston, MA, 1992.
(5) Traylor, T. G.; Tsuchiya, S.; Byun, Y.-S.; Kim, C. *J. Am. Chem. Soc.* **1993**, *115*, 2775−2781.
(6) Traylor, T. G.; Kim, C.; Richards, J. L.; Xu, F.; Perrin, C. L. *J. Am. Chem. Soc.* **1995**, *117*, 3468−3474.
(7) Cunningham, I. D.; Danks, T. N.; Hay, J. N.; Hamerton, I.; Gunathilagan, S. *Tetrahedron* **2001**, *57*, 6847−6853.
(8) Nam, W.; Jin, S. W.; Lim, M. H.; Ryu, J. Y.; Kim, C. *Inorg. Chem.* **2002**, *41*, 3647−3652.
(9) Cunningham, I. D.; Danks, T. N.; O'Connell, K. T. A.; Scott, P. W. *J. Chem. Soc., Perkin Trans. 2* **1999**, 2133−2139.
(10) Nam, W.; Lim, M. H.; Oh, S.-Y.; Lee, J. H.; Lee, H. J.; Woo, S. K.; Kim, C.; Shin, W. *Angew. Chem., Int. Ed.* **2000**, *39*, 3646−3649.
(11) Lee, K. A.; Nam, W. *Bull. Korean Chem. Soc.* **1996**, *17*, 669−671.
(12) Nam, W.; Oh, S.-Y.; Sun, Y. J.; Kim, J.; Kim, W.-K.; Woo, S. K.; Shin, W. *J. Org. Chem.* **2003**, *68*, 7903−7906.
(13) Nam, W.; Lim, M. H.; Lee, H. J.; Kim, C. *J. Am. Chem. Soc.* **2000**, *122*, 6641−6647.
(14) Cunningham, I. D.; Danks, T. N.; Hay, J. N.; Hamerton, I.; Gunathilagan, S.; Janczak, C. *J. Mol. Catal. A: Chem.* **2002**, *185*, 25−31.
(15) Lee, K. A.; Nam, W. *J. Am. Chem. Soc.* **1997**, *119*, 1916−1922.
(16) Nam, W.; Lee, H. J.; Oh, S.-Y.; Kim, C.; Jang, H. G. *J. Inorg. Biochem.* **2000**, *80*, 219−225.
(17) Nam, W.; Lim, M. H.; Lee, H. J.; Kim, C. *J. Am. Chem. Soc.* **2000**, *122*, 6641−6647.
(18) Traylor, T. G.; Xu, F. *J. Am. Chem. Soc.* **1990**, *112*, 178−186.
(19) Bruice, T. C. *Acc. Chem. Res.* **1991**, *24*, 243−249.
(20) Traylor, T. G.; Kim, C.; Richards, J. L.; Xu, F.; Perrin, C. L. *J. Am. Chem. Soc.* **1995**, *117*, 3468−3474.
(21) Traylor, T. G.; Kim, C.; Fann, W. P.; Perrin, C. L. *Tetrahedron* **1998**, *54*, 7977−7986.
(22) Traylor, T. G.; Xu, F. *J. Am. Chem. Soc.* **1987**, *109*, 6201−6202.
(23) Traylor, T. G.; Ciccone, J. P. *J. Am. Chem. Soc.* **1989**, *111*, 8413−8420.
(24) Traylor, T. G.; Fann, W.-P.; Bandyopadhyay, D. *J. Am. Chem. Soc.* **1989**, *111*, 8009−8010.
(25) Selke, M.; Sisemore, M. F.; Valentine, J. S. *J. Am. Chem. Soc.* **1996**, *118*, 2008−2012.
(26) Nam, W.; Park, S.-E.; Lim, I. K.; Lim, M. H.; Hong, J.; Kim, J. *J. Am. Chem. Soc.* **2003**, *125*, 14674−14675.
(27) Lim, M. H.; Jin, S. W.; Lee, Y. J.; Jhon, G.-J.; Nam, W.; Kim, C. *Bull. Korean Chem. Soc.* **2001**, *22*, 93−96.
(28) Collman, J. P.; Chien, A. S.; Eberspacher, T. A.; Brauman, J. I. *J. Am. Chem. Soc.* **2000**, *122*, 11098−11100.
(29) Nam, W.; Lim, M. H.; Moon, S. K.; Kim, C. *J. Am. Chem. Soc.* **2000**, *122*, 10805−10809.
(30) Moore, K. T.; Horvath, I. T.; Therien, M. J. *Inorg. Chem.* **2000**, *39*, 3125−3139.
(31) Fujii, H. *Coord. Chem. Rev.* **2002**, *226*, 51−60.
(32) Fujii, H. *Chem. Lett.* **1994**, 1491−1494.

of the mechanism and kinetics of iron porphyrin-catalyzed olefin and paraffin oxidations, a detailed analysis of the reaction kinetics has not been made for any porphyrin system.

Iron porphyrins halogenated on the periphery of the porphyrin ring or containing halogenated substituents attached to the porphyrin ring have been shown to be particularly efficient for both epoxidation and hydroxylation reactions.[35−37] Such porphyrins are also more resistant to degradation via free-radical attack than those containing electron-donating substituents.[1] These features have led a number of investigators to focus on iron(III) tetrakispentafluorophenyl porphyrin ($F_{20}$TPPFe(III)). In the presence of hydrogen peroxide, $F_{20}$TPPFe(III) can catalyze the epoxidation of olefins and the hydroxylation of both olefins and paraffins. The epoxidation of cyclooctene is particularly notable because only a single product, cyclooctene oxide, is produced, and for this reason, a number of studies have been devoted to understanding the mechanism of this process.[7,13−15]

Cunningham and co-workers have proposed that hydrogen peroxide reacts with $F_{20}$TPPFe(III) to produce an iron(III) hydroperoxo species, which then undergoes heterolytic O−O bond cleavage to form an iron(IV) $\pi$-radical cation species. The latter species then participates in two parallel reactions: the epoxidation of cyclooctene and the decomposition of hydrogen peroxide. The former reaction is taken to be very fast, while the later is taken to be fast. Both the pathways ultimately return the catalyst to its original iron(III) state.[7]

On the other hand, Nam and co-workers have suggested that the iron(IV) oxo species produced by the homolytic cleavage of iron(III) hydroperoxide species might also be involved in olefin epoxidation.[26] However, two observations argue against this idea. The first is that epoxidation of cis- and trans-stilbene occurs with retention of stereospecificity.[8] This result is strongly indicative of epoxidation via an iron(IV) $\pi$-radical cation, rather than by an iron(IV) oxo species, which would be expected to lead to a loss of stereospecificity.[5] The second observation is that even extremely small quantities of water suppress the epoxidation activity of iron(IV) oxo species.[26] Since water is always present together with hydrogen peroxide because reagent $H_2O_2$ is available as 30 wt % aqueous solution, the pathway via iron(IV) oxo species should be negligible.

A second issue is whether hydrogen peroxide decomposition occurs exclusively via the reaction of $H_2O_2$ with iron(IV) radical cations, as suggested by Cunningham and co-workers, or whether it involves iron(IV) oxo species, as well. If only one intermediate were involved in both the epoxidation of cyclooctene and the decomposition of hydrogen peroxide, then one would expect that at very high cyclooctene concentrations, the selectivity for the utilization of $H_2O_2$ for epoxidation would approach 100% asymptotically. Since this does not occur, it suggests that another intermediate, for example, the iron(IV) oxo species, might be involved in the decomposition of $H_2O_2$.

The aim of this work was to develop a more comprehensive picture of the mechanism and kinetics of cyclooctene epoxidation by hydrogen peroxide and the kinetics of hydrogen peroxide decomposition, catalyzed by $F_{20}$TPPFe(III). Particular attention was devoted to identifying the roles of solvent composition and reactant concentrations on the rates of both processes. A further objective was to determine rate coefficients and equilibrium constants for the elementary steps involved in cyclooctene epoxidation and hydrogen peroxide decomposition.

## Experimental Section

**Reagents.** Deuterium oxide, 99.9%, was obtained from Cambridge Isotope Laboratories, Inc. Cis-cyclooctene, 95%, was obtained from Alfa-Aesar. $F_{20}$TPPFe(III) in its chloride-ligated form and dodecane, 99+%, were obtained from Aldrich. Non-UV grade acetonitrile, 99.99%, methanol, 99.98%, ACS grade chloroform, 99.8%, and hydrogen peroxide, 30%, were all obtained from EMD Chemicals.

**Reactions.** Reactions were initiated by mixing 330 $\mu$L of cyclooctene, 2.75 mL of solvent (see below), 250 $\mu$L of a 1 mM solution of porphyrin dissolved in solvent, and 5.0 $\mu$L of hydrogen peroxide in a 5 mL reaction vial. Using these conditions, cyclooctene was in excess and hydrogen peroxide was the limiting reagent. Unless otherwise stated, the solvent used for all reactions consisted of 25 vol % methanol and 75 vol % acetonitrile. This choice of solvent composition was based on the need to keep the rate of reaction at a level that could be measured readily and yet maintain a relatively high yield of cyclooctene epoxide based on the consumption of hydrogen peroxide. By increasing the methanol concentration, it was also possible to decrease porphyrin degradation. To facilitate product analysis, 10 $\mu$L of dodecane was added as a standard to the reaction mixture. All reactions were performed at room temperature.

**Product Analysis.** The concentration of cyclooctene epoxide as a function of time was determined by gas chromatography. Analysis was carried out using an HP 6890 series gas chromatograph equipped with an Agilent DB Wax (30 m × 0.32 mm × 0.5 $\mu$m) capillary column and an FID detector. The 15 min required to analyze a single sample via gas chromatography was on the order of the time for the completion of the reaction. Therefore, multiple reactions were performed in order to obtain data points as a function of time. All data points were obtained at least in triplicate, and the repeatability of the data was always within ±2%. The repeatability of measuring cyclooctene epoxide via gas chromatography was determined to be within ±1% by analyzing a calibrated standard.

The hydrogen peroxide concentration was measured as a function of time using $^1$H NMR.[38] These analyses were carried out using a 400 MHz VMX spectrometer. Samples were prepared in 5 mL reaction vials as previously described with the exception that the catalyst was not added to the vial. A portion of this reaction mixture was transferred to a precision NMR tube. Chloroform was used as the internal standard for the NMR experiments. The reaction was initiated by adding a concentrated solution of $F_{20}$TPPFe(III) to the NMR tube prior to taking scans. An NMR spectrum was taken every 32 s by averaging the data from four scans. The area of the hydrogen peroxide peak, centered at 10.3 ppm, was then integrated and compared to the area of an internal standard. $^1$H NMR experiments were run in at least triplicate to verify the repeatability of the experiments; the experimental repeatability was approximately ±5%. The quantification of hydrogen peroxide via $^1$H NMR was shown to be accurate within ±2% by comparing the relative areas of the peroxide peak and the internal standard peak for calibrated standard solutions; multiple internal standards were used to verify the accuracy. The purity of the internal standard was taken as stated by the manufacturer, while the concentration of the standardized hydrogen peroxide solution was verified by a potassium permanganate titration.

**Porphyrin Analysis.** Degradation of the porphyrin species was quantified by UV−visible spectroscopy using a Varian Cary 400 Bio UV−visible spectrometer. Scans of the reacting system were taken as

(33) Almarsson, O.; Bruice, T. C. *J. Am. Chem. Soc.* **1995**, *117*, 4533−4544.
(34) He, G.-X.; Bruice, T. C. *J. Am. Chem. Soc.* **1991**, *113*, 2747−2753.
(35) Grinstaff, M. W.; Hill, M. G.; Labinger, J. A. *Science* **1994**, *264*, 1311−1313.
(36) Brinbaum, E. R.; Grinstaff, M. W.; Labinger, J. A.; Bercaw, J. E.; Gray, H. B. *J. Mol. Catal. A: Chem.* **1995**, *104*, L119−L122.
(37) Gross, Z.; Simkhovich, L. *Tetrahedron Lett.* **1998**, *39*, 8171−8174.
(38) Stephenson, N. A.; Bell, A. T. *Anal. Bioanal. Chem.* **2005**, *381*, 1289−1293.

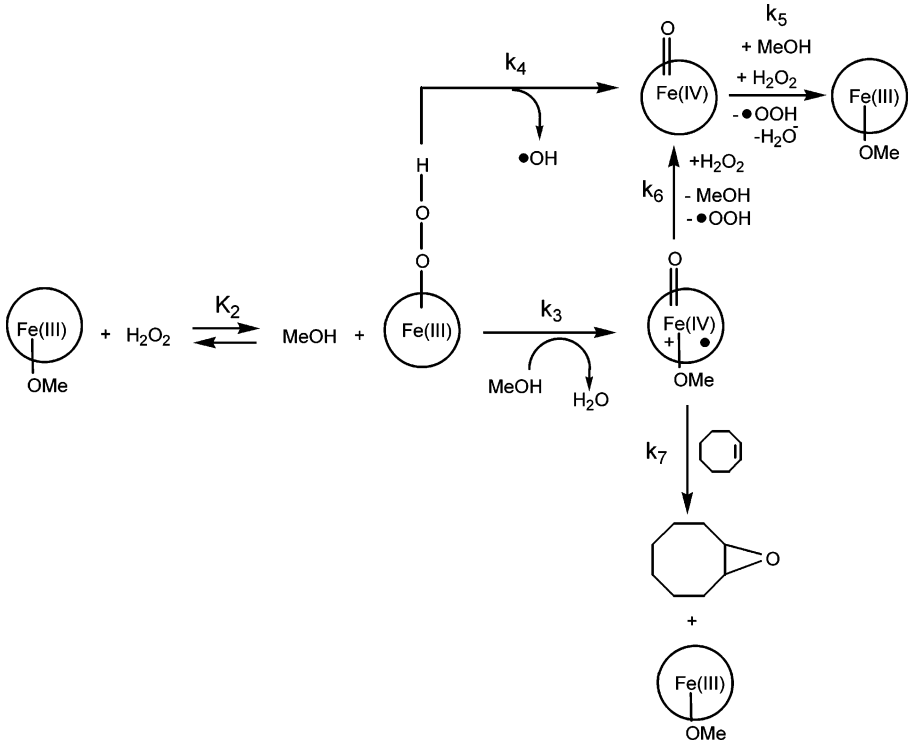


***Figure 1.*** The proposed mechanism for the epoxidation of cyclooctene using hydrogen peroxide as the oxidant and $F_{20}$TPPFe(III) as the catalyst.

a function of reaction time. The UV−visible spectra were then integrated to find the area under the peaks between 280 and 700 nm. An extinction coefficient was calculated based on a linear plot of integrated area versus porphyrin concentration. The porphyrin concentration versus reaction time was then fit empirically to a first-order exponential decay function. The repeatability of the UV−visible scans was shown to be better than ±2%. Negligible error was associated with taking repeated scans; all error was associated with the sample preparation.

Analyses of the porphyrin species were carried out using a 400 MHz VMX spectrometer. Concentrated porphyrin solutions (~17 mM) in acetonitrile/methanol solutions were analyzed. The spectral width was set to 75 188 Hz so that the $\beta$-pyrrole protons of the porphyrin could be monitored. NMR spectra of the porphyrin were collected by taking 256 scans.

## Proposed Mechanism and Method of Data Analysis

The proposed mechanism is shown in Figure 1. This scheme is similar to that presented by Cunningham and co-workers[7] in that epoxidation results from the reaction of cyclooctene with the $\pi$-radical cation formed via heterolytic cleavage of the oxygen−oxygen bond of the hydroperoxo intermediate (reaction 3). Cyclooctene epoxidation occurs via reaction 7. In distinction to the mechanism of Cunningham and co-workers, the mechanism shown in Figure 1 also includes a pathway for the homolytic cleavage of the hydroperoxo species (reaction 4). Hydrogen peroxide decomposition is envisioned to occur via reaction 5. Reaction 6 is included to account for the conversion of the iron(IV) $\pi$-radical cation to the iron(IV) oxo species. The participation of hydroperoxo species as intermediates in olefin epoxidation appears unlikely based on recent theoretical work, which shows that the activation energy for ethene epoxidation by hydroperoxo species is high (53 kcal/mol) compared to that for expoxidation by iron(IV) $\pi$-radical cations (14 kcal/mol).[39,40]

Much of the data for this research were collected before the $^1$H NMR technique had been developed for measuring the concentration of hydrogen peroxide in situ. To analyze such data required making a number of assumptions about the relationship of the rate of consumption of hydrogen peroxide relative to the rate of production of cyclooctene oxide, as well as an assumption about the concentration of catalyst during the course of the reactions. In what follows, we give a brief statement of the working assumptions and show how these can be used to determine an apparent first-order rate coefficient for the consumption of hydrogen peroxide, $k_{obs}$, and the yield of cyclooctene oxide based on the production of cyclooctene oxide.

The first assumption made in the derivation of an expression for $k_{obs}$ is that the percentage of iron(III) porphyrin axially ligated by methanol does not change with time. It was also assumed that the rate of reaction 7 is much faster than the rate of reaction 6, which leads to the expectation that the yield of cyclooctene oxide based on the amount of hydrogen peroxide consumed should be time independent. On the basis of the mechanism shown in Figure 1, the rate of epoxidation can be written according to eq 1. Making use of the pseudo-steady-state hypothesis for the iron(IV) $\pi$-cation intermediate and assuming that reaction 2 is equilibrated, eq 1 can be rewritten as eq 2. The concentration of $H_2O_2$ as a function of time can be determined from eq 3, which follows from the assumption that the ratio of heterolytic to homolytic cleavage is constant throughout the entire reaction combined with the fact that cyclooctene oxide is the only oxidation product. In this equation, $Y_\infty$ is the ratio of the amount of epoxide generated after all of the hydrogen peroxide has been consumed to the initial amount

(39) Kamachi, T.; Shiota, Y.; Ohta, T.; Yoshizama, K. *Bull. Chem. Soc. Jpn.* **2003**, *76*, 721−732.
(40) Ogliaro, F.; de Visser, S. P.; Cohen, S.; Sharma, P. K.; Shaik, S. *J. Am. Chem. Soc.* **2002**, *124*, 2806−2817.

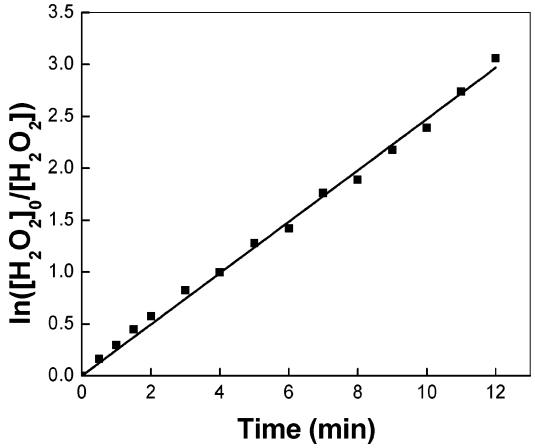


***Figure 2.*** Gas chromatography data allow for the graphical extraction of $k_3K_2$ and $k_4K_2$.

of hydrogen peroxide. Combining eqs 2 and 3, leads to eq 4, in which $k_{obs}$ is defined by eq 5. As shown in eq 6, integration of eq 4 gives the expression for hydrogen peroxide as a function time.

$$\frac{d[C_8 - O]}{dt} = k_7[+\bullet Fe(IV) = O][C_8] \quad (1)$$

$$\frac{d[C_8 - O]}{dt} = k_3K_2[Fe - OMe][H_2O_2] \quad (2)$$

$$[H_2O_2] = [H_2O_2]_0 - \frac{[C_8 - O]}{Y_\infty} \quad (3)$$

$$\frac{d[H_2O_2]}{dt} = -k_{obs}[H_2O_2] \quad (4)$$

$$k_{obs} = \frac{k_3K_2[Fe - OMe]}{Y_\infty} \quad (5)$$

$$\ln\left(\frac{[H_2O_2]_0}{[H_2O_2]}\right) = k_{obs}t \quad (6)$$

$$\text{Yield} = \frac{[C_8 - O]}{[H_2O_2]_0} \times 100\% \cong \frac{k_3[MeOH]}{k_3[MeOH] + 2k_4} \times 100\% \quad (7)$$

If all of the assumptions involved in the analysis are valid, then a plot of the logarithm of the ratio of the initial hydrogen peroxide concentration to that occurring at any time should be a linear function that passes through the origin. As seen in Figure 2, this is indeed the observed relationship. The individual assumptions underlying the definition of $k_{obs}$ are substantiated below. The value of $k_3K_2$ can be determined from the expression for $k_{obs}$ and the slope of the plot shown in Figure 2. A value for $k_4K_2$ can be estimated by making a few additional assumptions. If peroxide decomposition occurs only via the homolytic pathway and the ratio of the rate of homolytic to heterolytic cleavage is constant throughout the reaction, the final yield can be approximated by eq 7. A factor of 2 is placed before the $k_4$ term in the yield expression since two molecules of hydrogen peroxide are consumed in the homolytic pathway (see Figure 1).

In the next section, the experimental results are examined in light of the proposed mechanism and the method of data analysis presented above. This is then followed by a more detailed analysis of the kinetics of cyclooctene epoxidation and hydrogen peroxide decomposition in the presence and absence of cyclooctene. For that part of the discussion, data on the consumption of $H_2O_2$ were obtained from $^1H$ NMR analyses. It is also shown that the rate parameters obtained through the simplified analysis presented above and those obtained through the more detailed analysis are very similar.

## Results and Discussion

**Solvent Effects.** When acetonitrile or methylene chloride is used as the solvent, the porphyrin remains in its chloride-ligated form, and epoxidation does not occur. Epoxidation occurs once methanol is added to the aprotic solvents. It was also observed that in the absence of cyclooctene hardly any hydrogen peroxide decomposition occurred without the addition of methanol to the acetonitrile. Similar effects of solvent composition have been reported previously and have been attributed to replacement of the chloride ligand by an alkoxide.[10−12]

UV−visible spectroscopy was used to identify the effects of solvent composition on the nature of the axial ligand with the $F_{20}$TPPFe(III). In pure acetonitrile, a Soret peak is observed at 407 nm, which we assign to $F_{20}$TPPFe−Cl. When acetonitrile is progressively replaced by methanol, the Soret peak shifts to 388 nm and then to 404 nm. We assign the feature at 388 nm to the methoxide-ligated porphyrin, $F_{20}$TPPFe(III)−$OCH_3$, and the feature at 404 nm to $F_{20}$TPPFe(III)−$OCH_3$ interacting with a second molecule of methanol. We note that Lee and Nam have made a similar assignment for the band at 404 nm.[15]

Under reaction conditions, Soret bands are observed at 388 and 410 nm, but not at 404 nm, independent of the methanol concentration. We suggest that coordination of hydrogen peroxide at the proximal position of the porphyrin precludes the ligation of a second equivalent of methanol. After all hydrogen peroxide is consumed, UV−visible spectra of the reaction mixture indicate that bismethanol ligation is again possible, as evidenced by a Soret band at 404 nm. The intensity of the feature at 410 nm under reaction conditions varies strongly depending on whether cyclooctene is present or absent from the reaction mixture. This feature is assigned to overlapping bands due to $F_{20}$TPPFe(III)−Cl and an iron(IV) oxo species. The presence of the latter species is indicated by the appearance of a characteristic band at 540 nm.[11] When cyclooctene is present, the peak at 540 nm is absent, suggesting that the solution contains almost exclusively $F_{20}$TPPFe(III)−Cl and $F_{20}$TPPFe(III)−$OCH_3$. On the basis of this evidence, we propose that the active species for catalysis is $F_{20}$TPPFe−$OCH_3$, and that this species is present in equilibrium with $F_{20}$TPPFe−Cl defined by the following reaction:

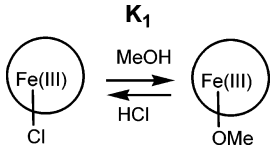


The equilibrium constant, $K_1$, associated with this reaction can be calculated from the relative concentrations of $F_{20}$TPPFe−Cl and $F_{20}$TPPFe−$OCH_3$, which are determined by deconvo-

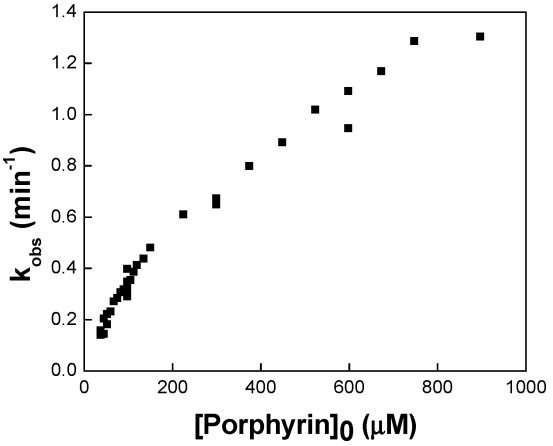


***Figure 3.*** Nonlinear relationship between the observed rate constant and the total porphyrin concentration.

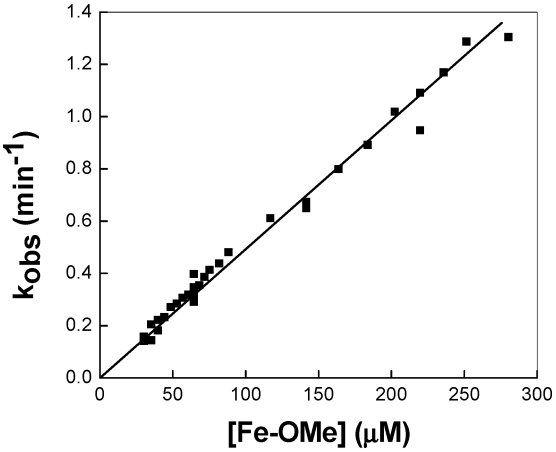


***Figure 4.*** Linear relationship between the observed rate constant and the methoxide-ligated porphyrin.

lution of the UV−visible spectrum taken under reaction conditions. By this means, a value of $K_1 = 1.3 \times 10^{-5}$ is obtained.

To test the ideas that only the methoxide-ligated porphyrin species are active for epoxidation and that $F_{20}$TPPFe−Cl and $F_{20}$TPPFe−$OCH_3$ are in equilibrium, the value of $k_{obs}$ was determined as a function of the total porphyrin concentration. On the basis of the aforementioned equilibrium relationship and material balances, one would expect the concentration of the methoxide-ligated porphyrin to increase nonlinearly with the concentration of total porphyrin. If the observed rate of reaction is first order in the methoxide-ligated porphyrin species, then the observed rate constant will also be nonlinear as a function of the total porphyrin concentration. As seen in Figure 3, this relationship is observed. However, Figure 4 shows that $k_{obs}$ is a linear function of $F_{20}$TPPFe−$OCH_3$; the concentration of which is determined by fitting the value of $K_1$ to the kinetic data shown in Figure 3; this fitting results in a value of $K_1 = 1.2 \times 10^{-5}$, which is comparable to that obtained from UV−visible spectroscopy ($1.3 \times 10^{-5}$), as described above. The very close agreement of the two values of $K_1$ obtained by independent means supports the proposition that the addition of methanol leads to the conversion of $F_{20}$TPPFe−Cl to $F_{20}$TPPFe−$OCH_3$.

$^1$H NMR was used to further substantiate the hypothesis that a change in the nature of the axial ligand on the porphyrin occurs as the percentage of methanol in the solvent is varied. Consistent with literature,[41,42] we found that the β-pyrrole protons of $F_{20}$TPPFe−Cl produce an NMR signal at 83 ppm in purely aprotic solvents (acetonitrile and $CDCl_3$). As methanol was substituted progressively for acetonitrile, the peak at 83 ppm decreased in magnitude, while a new peak appeared at 65 ppm and increased in magnitude. Both NMR peaks are broad and are located significantly downfield from the position of the β-pyrrole resonance for iron-free porphyrin. These observations are characteristic of a paramagnetic porphyrin species, suggesting no change in the spin state or oxidation state of the Fe cation occurs as methanol is substituted for acetonitrile. We attribute the peak at 65 ppm to the β-pyrrole protons of iron porphyrins in which methoxide anions serve as the axial ligand. This interpretation is consistent with previously reported observations of the effects of axial ligands on the $^1$H NMR shifts of paramagnetic Fe(III) porphyrins.[41] Since the methoxide anion is less electron withdrawing than the chloride anion, the electron density on the porphyrin ring will be higher in the former case. Consistent with this reasoning, the β-pyrrole resonance would be expected to shift upfield relative to that for the chloride-ligated porphyrin, which is what is observed. The presence of two distinct peaks at 83 and 65 ppm indicates an equilibrium relationship between the two species. Due to the high concentration of porphyrin required for NMR analysis and the rapid kinetics of the epoxidation reaction, the porphyrin catalyst could not be studied by NMR under reaction conditions. However, the above results do provide further evidence to support our claim of methoxide for chloride ligand substitution occurring upon progressive replacement of acetonitrile by methanol in the solvent.

The mechanism shown in Figure 1 suggests that methanol participates in the heterolytic cleavage of the iron−hydroperoxo intermediate in a manner analogous to that proposed for hydroperoxide species in the heme-containing enzyme, cytochrome P-450. In that system, the iron−hydroperoxo intermediate is converted to the ferryl porphyrin radical−cation intermediate via protonation and elimination of water. The proton is donated from a threonine unit on the enzyme; the process is also facilitated by several other amino acid derivatives on the enzyme.[43,44] Similar acid/base processes have been reported in model porphyrin systems, and it is thought that the acidic character of methanol facilitates the heterolytic cleavage of the oxygen−oxygen bond of the hydroperoxo−porphyrin intermediate when the solvent system contains methanol and an aprotic solvent.[18]

As shown in Figure 5, both the observed rate constant and the yield of epoxide based on hydrogen peroxide consumption increase with increasing methanol concentration. Heterolytic cleavage of the iron−hydroperoxo intermediate involves proton transfer between methanol and the hydroperoxo intermediate, while homolytic cleavage does not. If only heterolytic cleavage occurs, as suggested by Cunningham and co-workers,[7] then changing the methanol concentration should not affect the yield. The increase in yield and the increase in the observed rate constant strongly indicate that the pathways involving homolytic

(41) Birnbaum, E. R.; Hodge, J. A.; Grinstaff, M. W.; Schaefer, W. P.; Henling, L.; Labinger, J. A.; Bercaw, J. E.; Gray, H. B. *Inorg. Chem.* **1995**, *34*, 3625−3632.
(42) Song, B.; Park, B.; Han, C. *Bull. Korean Chem. Soc.* **2002**, *23*, 119−121.
(43) Meunier, B.; Bernadou, J. *Struct. Bonding* **2000**, *97*, 1−35.
(44) de Montellano, O. *Cytochrome P450: Structure, Mechanism, and Biochemistry*, 2nd ed.; Plenum Press: New York, 1995.

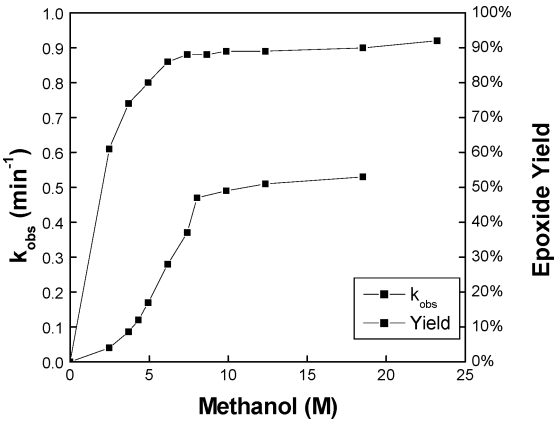


***Figure 5.*** Observed rate constant and epoxide yield as a function of methanol concentration.

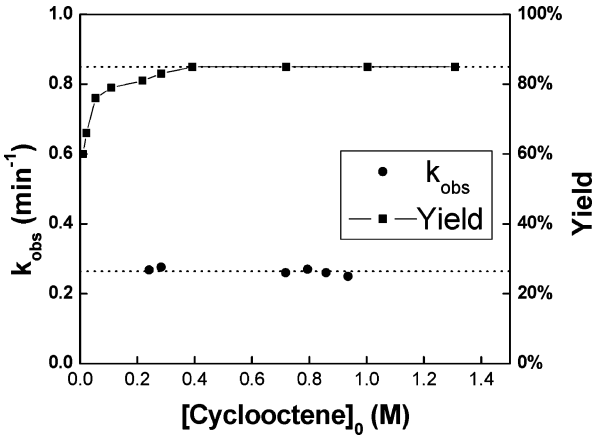


***Figure 6.*** Yield and observed rate constant as a function of substrate concentration.

and heterolytic cleavage of the O−O bond in iron(III) hydroperoxo species compete. Even though the dependence on methanol concentration disappears from the expression for $k_{obs}$ when the pseudo-steady-state hypothesis is applied, the observed rate constant continues to be a function of methanol concentration because of the dependence on the concentration of methoxide-ligated porphyrin.

The proposed mechanism (see Figure 1) should also explain the sigmoidal behavior of the observed rate constant as the methanol concentration increases. This type of relationship has been reported before for $F_{20}$TPPFe(III) in protic solvents, although not interpreted.[12] As would be expected based on the proposed mechanism, the observed rate constant plateaus at higher methanol concentrations. The proposed equilibrium relationship between the chloride and methoxide-ligated species predicts a hyperbolic increase in the amount of methoxide-ligated porphyrin present. The simultaneous saturation of the concentration of the methoxide-ligated porphyrin species and the observed rate constant at high methanol concentrations support the idea that only the methoxide-ligated species are active for catalysis. However, below 32 vol % methanol, the observed rate constant does not increase hyperbolically as would be expected based only on the amount of methoxide-ligated porphyrin present in the system. Instead, $k_{obs}$ appears to increase as the square of the methanol concentration. This suggests that methanol may play some other role in the equilibrium reaction between the methoxide-ligated porphyrin or in the cleavage of the O−O bond of the iron(III) hydroperoxo species.

Several factors can be proposed to account for the observed reaction rate being lower than would be predicted based on the amount of methoxide-ligated porphyrin present. First, at lower methanol concentrations, a higher percentage of the porphyrin will be in the iron(IV) oxo form at steady-state reaction conditions. If the amount of porphyrin in the iron(IV) oxo state became significant relative to the total porphyrin concentration, then less porphyrin would be in the methoxide-ligated state under reaction conditions, thus lowering the observed rate of reaction. Second, porphyrin degradation increases as the methanol concentration decreases. If a significant amount of porphyrin is degraded during the initial few minutes of the reaction, then the assumption that the concentration of methoxide-ligated porphyrin is constant over the interval in which the rate data are collected will be invalid, resulting in a lower observed rate constant. Finally, the cleavage of the oxygen−oxygen bond in hydrogen peroxide may be a complex function of the interactions between the solvent system and the hydrogen peroxide molecules. A process that would be consistent with the observed phenomenon is the interaction of two methanol molecules with a single molecule of hydrogen peroxide via hydrogen bonding. Such an interaction could result in weakening the oxygen−hydrogen bonds in the hydrogen peroxide molecule, thus facilitating cleavage of the O−O bond of the hydroperoxide ligand. Consistent with this hypothesis, we observed that the position of the proton NMR peak for hydrogen peroxide shifts downfield as the amount of methanol in the reaction mixture is increased; this trend is indicative of an increase in the extent of hydrogen bonding.

**Substrate Concentration.** If the mechanism proposed in Figure 1 is valid, both the yield of epoxide and $k_{obs}$ should be independent of the initial cyclooctene concentration at high substrate concentrations. Figure 6 shows that both expectations are borne out for cyclooctene concentrations between 0.4 and 1.4 M. This indicates that over this range of cyclooctene concentrations the rate of reaction 7 is much greater than the rate of reaction 6, and that reaction 3 is irreversible. The fact that the observed rate of epoxide formation does not change with increasing cyclooctene concentration confirms the application of the pseudo-steady-state hypothesis to the intermediate formed via heterolytic cleavage of the iron(III) hydroperoxide species formed upon the initial interaction of $H_2O_2$ with the catalyst.

To obtain more information about the relative values of $k_6$ and $k_7$, the initial cyclooctene concentration was decreased until the rates of reactions 6 and 7 became comparable, as evidenced by a reduction in the epoxide yield. Figure 6 shows that the yield of epoxide decreased noticeably once the cyclooctene concentration was decreased below 0.1 M. On the basis of the model of the reaction kinetics, described below, the value of $k_6$ is determined to be 0.3 of that of $k_7$.

**Oxidant Concentration.** In the proposed mechanism shown in Figure 1, it is assumed that the rate of cyclooctene epoxidation is first order in hydrogen peroxide concentration, in agreement with what has been reported previously.[7,18] Several experiments were carried out to verify this assumption. As seen in Figure 7, neither the observed rate constant nor the final yield of epoxide relative to hydrogen peroxide consumed changes as the initial concentration of hydrogen peroxide is varied. Therefore, consistent with the proposed mechanism and the underlying

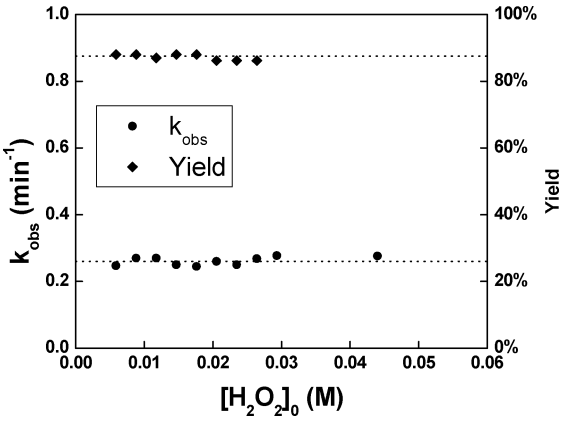


***Figure 7.*** Yield and observed rate constant as a function of $H_2O_2$.

***Table 1.*** Fitted Parameters for Porphyrin Decomposition Kinetics

| $[H_2O_2]_0$ (mM) | $y_0$ ($\mu$M) | $y_f$ ($\mu$M) | $\tau$ (s) |
|---|---|---|---|
| 2.9 | 8.9 | 3.5 | 0.44 |
| 2.9 | 11.9 | 7.4 | 0.35 |
| 2.9 | 14.9 | 11.0 | 0.27 |
| 2.9 | 17.9 | 14.5 | 0.20 |
| 2.9 | 20.9 | 17.9 | 0.16 |
| 2.9 | 23.9 | 21.1 | 0.13 |
| 2.9 | 26.9 | 24.3 | 0.11 |
| 2.9 | 14.9 | 11.0 | 0.27 |
| 4.4 | 14.9 | 10.0 | 0.26 |
| 5.9 | 14.9 | 9.3 | 0.24 |
| 7.3 | 14.9 | 7.5 | 0.27 |

assumptions, the production of cyclooctene epoxide is first order in hydrogen peroxide.

**Porphyrin Degradation.** Quantification of the porphyrin before and after the reaction using UV−visible spectroscopy showed that only 10% of the porphyrin was destroyed during the reaction, confirming that the total porphyrin concentration is approximately constant, as was assumed in order to determine $k_{obs}$ from the gas chromatographic data.

To develop a better representation of the kinetics of cyclooctene epoxidation, the kinetics of porphyrin decomposition were determined. UV−visible spectroscopy was used to measure the concentration of porphyrin as a function of time for different initial concentrations of porphyrin and hydrogen peroxide. Good fits to the data could be obtained using the expression

$$\frac{y - y_f}{y_0 - y_f} = \exp(-t/\tau) \qquad (8)$$

where $y_0$, $y$, and $y_f$ are the porphyrin concentrations at $t = 0$, at time $t$, and at the point when all of the hydrogen peroxide has been consumed, respectively. The parameter $\tau$ in eq 8 is the apparent time constant for porphyrin degradation. Values of $y_f$ and $\tau$ are shown in Table 1 for different values of the initial concentrations of porphyrin and hydrogen peroxide. It is evident that for a fixed initial concentration of hydrogen peroxide, the extent of porphyrin degradation decreases as the initial concentration of porphyrin increases, and that the time constant for porphyrin degradation decreases. On the other hand, for a fixed initial concentration of porphyrin, the extent of porphyrin degradation increases with an increase in the initial concentration of hydrogen peroxide, but the time constant for porphyrin degradation remains essentially constant.

While the decomposition of $F_{20}$TPPFe(III) during the oxidation of hydrocarbons by hydrogen peroxide has been reported previously,[7] a clear picture of the degradation mechanism is not available. Cunningham and co-workers propose that porphyrin degradation occurs via attack of the porphyrin ring by hydroxyl radicals.[7] This idea is supported by both theoretical[45] and experimental work[46] indicating that the porphyrin ring in the biological heme oxygenase system degrades via a radical mechanism. In our work, the participation of radicals is supported by the observation that porphyrin degradation is reduced in the presence of acetone and dimethyl sulfoxide, both of which are known to be radical traps.[47−49] For example, when the reaction was carried out in an acetonitrile/methanol mixture containing less than 10 vol % methanol, all of the porphyrin was destroyed by the end of the experiment, even though hydrogen peroxide remained. When the acetonitrile was replaced with acetone, the porphyrin was protected from complete degradation, and the reaction stopped upon complete consumption of the hydrogen peroxide.

A porphyrin degradation mechanism involving free radicals would explain the results presented in Table 1. Radical species (e.g., •OOH, •OH) formed during reaction can follow several pathways. Two of the major possibilities are attack on the porphyrin ring and radical−radical recombination. As the porphyrin catalyst concentration is increased, the rate at which radicals are produced will increase, as well. If porphyrin degradation is first order in radical species and radical recombination is second order in radical species, then the rate of radical recombination will increase faster than the observed rate of porphyrin decomposition as the initial porphyrin concentration is increased. Less porphyrin is consumed as the porphyrin concentration is increased because a higher radical concentration favors second-order radical recombination as opposed to first-order porphyrin decomposition. The apparent time constant, $\tau$, characterizes the duration over which radicals are produced in the system. Since radicals are derived from hydrogen peroxide, $\tau$ characterizes the time constant for the consumption of hydrogen peroxide. As expected for a catalyzed reaction, the time required to consume all of the peroxide decreases as the porphyrin catalyst concentration increases. Therefore, the time constant, $\tau$, should decrease as the porphyrin catalyst concentration increases. This explanation would also predict that $\tau$ would be independent of the initial hydrogen peroxide concentration since the oxidation reactions shown in Figure 1 are first order in hydrogen peroxide. As shown in Table 1, $\tau$ behaves as predicted by the proposed radical mechanism. In addition, the amount of porphyrin degraded should increase with an increase in the initial concentration of hydrogen peroxide since more radicals will be produced. The results shown in Table 1 are consistent with this expectation.

## Kinetic Modeling

**Results.** A detailed analysis of the kinetics of cyclooctene epoxidation and hydrogen peroxide decomposition was carried

(45) Sharma, P. K.; Kevorkiants, R.; de Visser, S. P.; Kumar, D.; Shaik, S. *Angew. Chem., Int. Ed.* **2004**, *43*, 1129−1132.
(46) Wilks, A.; Torpey, J.; Ortiz de Montellano, P. R. *J. Biol. Chem.* **1994**, *269*, 29553−29556.
(47) Scaduto, R. C. *Free Rad. Biol. Med*. **1995**, *18*, 271−277.
(48) Roelfes, G.; Lubben, M.; Hage, R.; Que, L.; Feringa, B. L. *Chem.—Eur. J.* **2000**, *6*, 2152−2159.
(49) Walling, C.; El-Taliawi, G. M. *J. Am. Chem. Soc.* **1973**, *95*, 844−847.

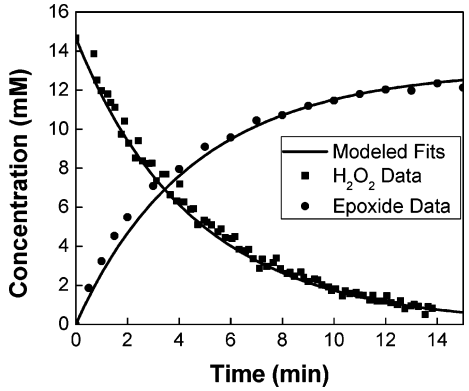


***Figure 8.*** Kinetic model for the case where cyclooctene is present.

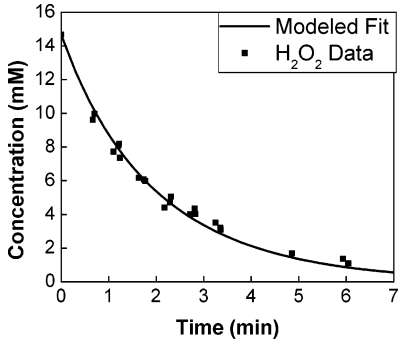


***Figure 9.*** Kinetic modeling for peroxide decomposition by $F_{20}$TPPFe(III).

out based on the mechanism presented in Figure 1. Differential equations representing the kinetics of cyclooctene epoxide formation and hydrogen peroxide consumption were written based on the proposed mechanism, and these equations were solved numerically using a fourth-order Runge−Kutta algorithm. To extract the parameters $k_3K_2$, $k_4K_2$, and $k_5$, the changes with time in the concentrations of cyclooctene and hydrogen peroxide predicted by the model were fitted to the experimental data taken in the presence and absence of cyclooctene. The method of least squares was used to fit the rate parameters to the data. The concentration of the methoxide-ligated porphyrin species was determined from the previously described equilibrium relationship. The total porphyrin concentration was represented using eq 8. The time constant for the porphyrin degradation was assumed to be identical to the time constant for peroxide consumption for both cases with and without cyclooctene present, and the amount of porphyrin remaining after the reaction was determined by UV−visible spectroscopy. Upon fitting the data, the best-fit values obtained were $k_3K_2 = 73\ M^{-1}\ s^{-1}$, $k_4K_2 = 32\ M^{-1}\ s^{-1}$, and $k_5 = 37\ M^{-2}\ s^{-1}$. Figures 8 and 9 show that the model does an excellent job of describing the data. It is also noted that the values of $k_3K_2$ and $k_5$ are consistent with those estimated by Cunningham and co-workers, which are on the order of 100 $M^{-1}\ s^{-1}$.[12] Note, $k_5$ should be multiplied by the methanol concentration (6.2 M) to be consistent with the observed rate constant predicted by Cunningham.

**Qualitative Comparison to UV−Visible Data.** The iron(IV) oxo intermediate formed by homolytic cleavage of the oxygen−oxygen bond of the iron(III) hydroperoxo species can be identified by a Soret peak at 410 nm and a second peak at 540 nm.[11] Deconvolution of the UV−visible data taken under reaction conditions to determine the relative amounts of each porphyrin species present is not feasible due to the close

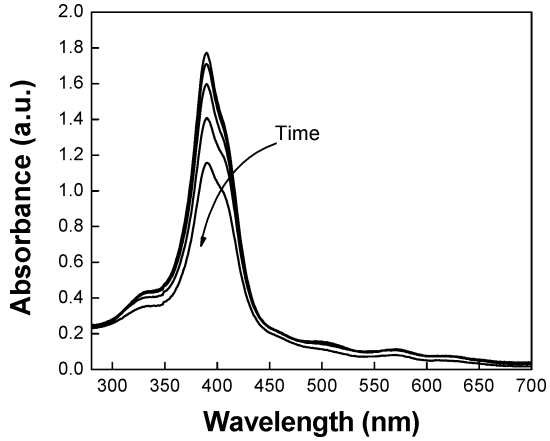


***Figure 10.*** UV−visible spectra under reaction conditions with cyclooctene present.

proximity of the Soret peaks for each porphyrin species. However, the UV−visible spectroscopy can be used to demonstrate qualitative agreement between the mechanism shown in Figure 1 and experimental observation. It should be noted that the same ratio of substrate, catalyst, and oxidant were used for the UV−visible experiments as were used for the reaction experiments; however, the concentrations of each species were reduced by a factor of 5 to prevent saturation of the detector. Under reaction conditions with cyclooctene present, the model predicts that 1% of the total porphyrin should be present as the iron(IV) oxo species. As seen in Figure 10, the lack of a significant contribution to the Soret peak at 410 nm suggests that the concentration of the iron(IV) oxo species is low when reaction occurs in the presence of cyclooctene. The shoulder on the Soret peak near 407 nm is attributed to the chloride-ligated porphyrin.

According to the mechanism presented in Figure 1, a higher concentration of iron(IV) oxo species should be present when cyclooctene is absent than when it is present since the iron(IV) oxo intermediate will also be produced via reaction 6, and reaction 7 will not consume the iron(IV) $\pi$-radical species. Since the rate of heterolytic cleavage is about 15 times greater than that of homolytic cleavage, a significant amount of the iron(IV) oxo species should be generated. The model of the reaction kinetics predicts that about 17% of the total porphyrin present will be in the iron(IV) oxo state. Figure 11 shows that there is a noticeable contribution to the spectrum around 410 nm, indicating that the iron(IV) oxo species are indeed present in a significant concentration under reaction conditions. Further confirmation of this interpretation is the clear evidence of a band at 540 nm. The chloride-ligated porphyrin species are also expected to contribute to this peak at 410 nm (see above). The kinetic model predicts that the latter species should correspond to 33% of the total porphyrin concentration. Thus, one would expect the Soret peaks at 388 and 410 nm to have similar magnitudes, assuming the extinction coefficients of all species to be similar. As seen in Figure 11, the UV−visible spectrum observed in the absence of cyclooctene is qualitatively consistent with the predictions of the model.

**Comparison of Techniques.** The rate coefficients extracted from the gas chromatographic data and from fitting the predictions of the kinetic model to both the gas chromatography and NMR data are in excellent agreement. On the basis of chromatographic data for cyclooctene oxide generation,

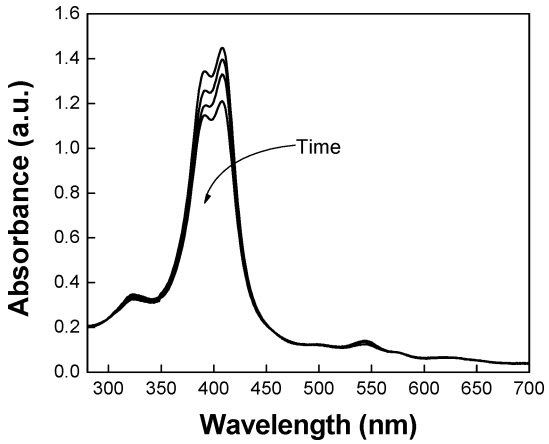


***Figure 11.*** UV−visible spectra under reaction conditions without cyclooctene present.

$k_3K_2 = 80 \pm 8$ $M^{-1}$ $s^{-1}$ and $k_4K_2 = 34 \pm 4$ $M^{-1}$ $s^{-1}$, respectively, and on the basis of the model of the kinetics, $k_3K_2 = 73 \pm 5$ $M^{-1}$ $s^{-1}$ and $k_4K_2 = 32 \pm 3$ $M^{-1}$ $s^{-1}$, respectively. This agreement validates the assumptions required to use the gas chromatography data alone for the determination of rate parameters and, most importantly, the assumption that the ratio of heterolytic to homolytic cleavage is constant throughout the course of the reaction and can be determined from the final yield. However, NMR data must be used if the value of $k_5$ is to be determined.

Finally, rather than assume that a constant percentage of the porphyrin is methoxide-ligated, the equilibrium relationship was used in the model to predict the concentration of methoxide-ligated porphyrin as a function of time. The model of the reaction kinetics predicts that approximately 61% of the porphyrin species is in the methoxide-ligated form over the time scale of the reaction; this is in agreement with the assumption that was used in the analysis of the gas chromatography data, namely, that the amount of porphyrin that is methoxide-ligated does not change significantly with time. On the basis of UV−visible data under reaction conditions, 62% of the porphyrin is in the methoxide-ligated state when the solvent mixture contains 25 vol % methanol.

## Conclusions

A mechanism has been proposed and verified for the epoxidation of cyclooctene by hydrogen peroxide using $F_{20}$TPPFe(III) as the catalyst. Epoxidation is found to involve an iron(IV) $\pi$-radical cation, but hydrogen peroxide decomposition involves an iron(IV) oxo species. To become active, the chloride-ligated form of the catalyst must first be converted into a methoxide-ligated form. A model of the reaction kinetics based on the mechanism presented in Figure 1 was used to determine the rate coefficients for three of the significant reactions steps; the equilibrium constant between the chloride-ligated and methoxide-ligated forms of porphyrin was also determined.

**Acknowledgment.** This work was supported by the Director, Office of Basic Energy Sciences, Chemical Sciences Division of the U.S. Department of Energy under Contract DE-AC03-76SF00098.

JA043380N